Received: 23 October 2019 | Revised: 20 December 2019 | Accepted: 10 January 2020

DOI: 10.1111/iwj.13314

ORIGINAL ARTICLE

IWJ WILEY

Biological dermal templates with native collagen scaffolds provide guiding ridges for invading cells and may promote structured dermal wound healing

Veronika Dill[1] | **Matthias Mörgelin**[1,2]

[1]Department of Clinical Sciences, Division of Infection Medicine, Lund University, Lund, Sweden

[2]Colzyx AB, Lund, Sweden

Correspondence
Matthias Mörgelin, Colzyx AB, Medicon Village, Lund SE-223 81, Sweden.
Email: matthias.morgelin@colzyx.com

Funding information
Stiftelsen för Strategisk Forskning, Grant/Award Number: K2014-56X-13413-15-3; Vetenskapsrådet, Grant/Award Number: 7480; Lund University; Memorial Fund; Swedish Foundation for Strategic Research; Swedish Research Council

Abstract

Dermal substitutes are of major importance in treating full thickness skin defects. They come in a variety of materials manufactured into various forms, such as films, hydrocolloids, hydrogels, sponges, membranes, and electrospun micro- and nanofibers. Bioactive dermal substitutes act in wound healing either by delivery of bioactive compounds or by being constructed from materials having endogenous activity. The healing success rate is highly determined by cellular and physiological processes at the host-biomaterial interface during crucial wound healing steps. Hence, it is important to design appropriate wound treatment strategies with the ability to work actively with tissues and cells to enhance healing. Therefore, in this study, we investigated biological dermal templates and their potential to stimulate natural cell adherence, guidance, and morphology. The most pronounced effect was observed in biomaterials with the highest content of native collagen networks. Cell attachment and proliferation were significantly enhanced on native collagen scaffolds. Cell morphology was more asymmetrical on such scaffolds, resembling native in vivo structures. Importantly, considerably lower expression of myofibroblast phenotype was observed on native collagen scaffolds. Our data suggest that this treatment strategy might be beneficial for the wound environment, with the potential to promote improved tissue regeneration and reduce abnormal scar formation.

KEYWORDS

bioactive dermal template, cell adherence, cell proliferation, native collagen scaffold, structured healing

1 | INTRODUCTION

Skin acts as an anatomical protective barrier between the external environment and internal organ system, to provide protection against pathogens, regulate body temperature, provide sensation, synthesise Vitamin D, and so on. Damage of skin tissue often results in infection, loss of proper tissue function, and scar formation, which ultimately becomes a major health care challenge.[1] Wound healing is a complex process divided into different stages – haemostasis, inflammation, proliferation, and remodelling of the regenerated tissue. These stages are characterised by carefully orchestrated sequences of cellular and molecular events including chemotaxis or signalling, phagocytosis, neocollagenesis, and remodelling of collagen matrix.[2] Moreover, during wound healing, regeneration and repairing are two different important aspects of functional tissue/organ formation. Without regeneration, repairing of injured tissue results

in scar formation or fibrosis.[3] The ever-increasing need for optimal full-thickness wound management initiated the development of appropriate dermal substitutes[1,4] to receive dermal regeneration.

There are different properties a dermal substitute has to fulfil to enhance tissue regeneration. Dermal substitutes should provide an artificial dermal matrix that allows for ingrowth by endogenous cells and reorganisation of replacement tissue by endogenous cells. Specifically, for biodegradable natural materials, their degradation needs to follow the dynamics of the wound repair, guaranteeing the physiological healing evolution, and releasing active principles when needed.[5] One class of dermal substitutes consists of purified biological molecules like collagen, which can be supplemented with, for example, glycosaminoglycans or elastin and also cross-linked in order to control its properties.[6]

Collagen is the most abundant mammalian protein, which provides mechanical strength to tissues and stimulates cell adhesion and proliferation.[7,8] High biocompatibility and biodegradability make collagen ideal for biomedical applications.[9,10] The fibrous collagen network facilitates cell migration to the wounded site, actively supporting wound healing.[11] Collagen-based dermal templates have been applied to cover burn wounds, treat ulcers,[12-15] reduce tissue contraction and scarring, and increase epithelialisation rate.[16] The multifunctional platform showed a favourable topography for cell proliferation and tissue vascularization, thus accelerating healing and wound closure. Despite their rather extensive usage as biomaterials for scaffold design, collagen scaffolds remain sustainable materials with highly engineering potential.

In the present study, we were prompted to explore whether native collagen networks can promote superior cell adhesion and proliferation on the surface of different commercially available dermal templates. Using an integrated approach, combining established methods with immunoelectron microscopy, we describe for the first time that biological dermal templates expose native collagen networks on their surface and display a pronounced potential to provide a versatile, multifunctional, and appropriate extracellular environment, able to actively promote natural tissue regeneration.

Key Messages

- successful wound healing depends on carefully orchestrated cellular and physiological processes at the host-biomaterial interface
- in this study, we investigated biological dermal templates and their potential to stimulate natural cell adherence, guidance, and morphology
- cell attachment and proliferation were significantly enhanced on native collagen scaffolds, and cell morphology was more asymmetrical on such scaffolds, resembling native in vivo structures. Importantly, considerably lower expression of myofibroblast phenotype was observed on native collagen scaffolds

2 | EXPERIMENTAL PROCEDURES

2.1 | Materials

Integra® Dermal Regeneration Template (bovine Collagen glycosaminoglycan, abbreviation: C-GAG) was purchased from Integra LifeSciences, Pelnac Dermal Substitute (porcine Collagen, abbreviation: C) from Eurosurgical Ltd, and MatriDerm® (bovine Collagen elastin, abbreviation: C-E) from MedSkin Solutions Dr. Suwelack AG. Skin biopsies were obtained from patients after informed written consent, according to protocols approved by the ethics committee at Lund University and in accordance with the Declaration of Helsinki Principles as described in[17]]. Rabbit polyclonal antibody against collagen III (ab7778), rabbit polyclonal antibody against collagen V (ab7046) and rabbit polyclonal antibody against alpha smooth muscle actin (ab5694) were purchased from Abcam PLC, Cambridge, UK.

2.2 | Transmission electron microscopy

samples were punched out to 5 mm diameter discs and incubated in PBS for 15 minutes at 4°C for rehydration. They were then fixed with 2.5% glutaraldehyde in 0.1 M sodium cacodylate, pH 7.4 (cacodylate buffer), washed with cacodylate buffer and dehydrated with an ascending ethanol series as described recently.[18] Specimens were then embedded in Epon 812 and cut into ultrathin sections on a Reichert Ultracut S ultramicrotome, Leica Microsystems, Wetzlar, Germany. They were examined at the Core Facility for Integrated Microscopy (CFIM), Panum Institute, Copenhagen University, in a Philips/FEI CM100 BioTWIN transmission electron microscope, and at the BioEM Lab, Biozentrum, University of Basel, in a Philips/FEI T12 transmission electron microscope. Images were recorded with a side-mounted Olympus Veleta camera and the ITEM acquisitions software.

2.3 | Scanning electron microscopy

punched out samples were prepared as described earlier and then fixed with 2.5% glutaraldehyde in cacodylate

buffer. They were washed with cacodylate buffer and dehydrated with an ascending ethanol series as described.[18] The specimens were then subjected to critical-point drying with carbon dioxide and absolute ethanol was used as an intermediate solvent. They were mounted on aluminium holders, sputtered with 20 nm palladium/gold, and examined in a Philips/FEI XL 30 field emission scanning electron microscope (FESEM) operated at 5 kV accelerating voltage.

2.4 | Immunoelectron microscopy

The binding properties and cellular architecture of keratinocytes and fibroblasts on the different collagen matrices were assessed by transmission immunoelectron microscopy as described previously.[19] Briefly, sections mounted on nickel grids were subjected to antigen retrieval with sodium metaperiodate and washed and blocked with 50 mM glycine. They were then incubated for 15 minutes with 5% goat serum in 0.2% BSA-c in PBS (pH 7.6), and then incubated overnight at 4°C with the rabbit polyclonal antibody against alpha smooth muscle actin (1:80 dilution). Next, grids were washed, incubated for 2 hours at 4°C with 10 μg/mL anti-rabbit gold-labelled IgG conjugate (BBI Solutions, Cardiff, UK), and washed and post-fixed in 2% glutaraldehyde. Finally, sections were washed with water and post-stained with 2% uranyl acetate and lead citrate. In some experiments, specimens were examined by negative staining, immunolabelling, and transmission electron microscopy (TEM). Samples were incubated for 30 minutes at 4°C with gold-labelled polyclonal rabbit antibodies against collagen III and V, adsorbed to 400-mesh carbon-coated copper grids and stained with 0.75% (w/v) uranyl formate as recently described in detail.[20] Specimens were examined in a Philips/FEI CM 100 TWIN (CFIM), or in a Philips/FEI T12 (C-CINA) transmission electron microscope as described earlier.

2.5 | Cells and culture conditions

Keratinocytes (Human Epidermal Keratinocytes, adult [HEKa], C-005-5C, Gibco) and fibroblasts (Human Dermal Fibroblasts, adult [HDFa], C0135C, Gibco) were purchased from Thermo Fisher Scientific, Waltham, MA. Cryopreserved cells were thawed according to the manufacturer's protocol and seeded on three 75 mL tissue culture flasks, each containing 15 mL of keratinocyte basal medium (KBM; KBM Gold, Lonza Group AG, Basel, Switzerland). The medium was supplemented with transferrin, recombinant human epidermal growth factor (rhEGF), bovine pituitary extract (BPE), antibiotics (Gentamycin: GA-1000), insulin, epinephrine, and hydrocortisone (PeproTech, NJ). For fibroblasts complete growth medium consisting of Dulbecco's modified eagle medium (D-MEM) with 100 mM sodium pyruvate (PAA Laboratories, Pasching, Austria), supplemented with 10% foetal bovine serum (FBS) (PAA Laboratories, Pasching, Austria) and 2 mM L-glutamine (Invitrogen, Carlsbad, CA), was used. Medium was changed every day and substituted with additional rhEGF at a final dilution of 1:1000. The cells were incubated for 7 days until they reached confluency. The cells were harvested by trypsinization (TrypLETM Select [1x], Life Technologies Corporation, Carlsbad, CA) and transferred into freezing medium, containing 1% BSA (Sigma Aldrich, St. Louis, MO) and 10% DMSO (Sigma-Aldrich, St. Louis, MO). One millilitre of aliquots of the cell suspension was transferred into cryotubes. The cryotubes were transferred to the freezer at −80°C for 24 hours and then finally stored in liquid nitrogen until further use.

2.6 | Cell attachment, cell spreading, and cell proliferation

Cells were gently thawed and counted in a haemocytometer using trypan blue (Fisher Scientific, Waltham, MA) to estimate the number of live/dead cells. They were finally diluted in appropriate media to final cell concentrations of 16 700 viable cells/mL. Three hundred microlitres of cell solution were added on top of punched out wound matrix samples, followed by incubation at 37°C for different times. Growth medium was replaced every other day. After the desired incubation time, growth medium was removed and the cells were gently washed twice with PBS. The cells were then fixed by the addition of 4% formaldehyde in PBS, followed by incubation at 4°C for 20 minutes. Finally, cells were rinsed three times in PBS and stored in 3 mL PBS until further evaluation.

2.7 | Cell alignment, elongation, and circularity

To determine the extent of cell elongation and alignment on different wound matrices, as well as cell elongation, at least 50 images of each sample were randomly captured on at least 30 different locations. By this means a total amount of 300 cells per group were evaluated in an objective manner. Cell alignment to wound matrix surface structures was investigated by manually measuring the angle between the tangent of visible fibrillar collagen structures in a given wound matrix, and a line along the longitudinal axis of each cell. Cell elongation was measured as the quotient of the longest possible line perpendicular to each cell, and the longest possible line along the longitudinal axis of the cell. Cell circularity was

determined as the quotient between cell area and cell perimeter^2, multiplied by 4π.

2.8 | Statistical analysis

Student's *t* test for paired data was performed to determine statistical significance. Values were expressed as means ± SE bars in the histograms. Statistical significances are expressed as n.s. ($P \geq .05$); * ($P \leq .05$); ** ($P \leq .01$); *** ($P \leq .005$).

3 | RESULTS

3.1 | Ultrastructural features of different biological dermal templates

Our recent findings demonstrated that collagen nativity influences important properties like protease binding and inactivation in chronic wounds. Prompted by the fact that the most native collagen matrices showed the strongest effect,[18] we wished to investigate these properties in further detail for collagen-based dermal templates.

An integrated electron microscopy approach was assessed to combine high-resolution FESEM, TEM, and immunoelectron microscopy. In a set of experiments, specimens were prepared for scanning electron microscopy, either as dry materials or after preincubation in physiological saline. They were compared with dermis areas in native human skin biopsies (Figure 1A, green pseudocolour). FESEM showed that C-E contained large amounts of three-dimensional fibrillar collagen networks (Figure 1C,G). Upon closer inspection at high resolution, the collagen fibrils exhibited the same appearance and three-dimensional supramolecular assemblies as intact collagen seen in dermis (Figure 1B,F). In contrast, in C-GAG (Figure 1D,H) and C (Figure 1E,I), comparably moderate amounts of fibrillar structures were visualised. These fibrillar structures appeared embedded in layers of somewhat amorphous sheets.

Similar observations were made by negative staining and TEM. Human skin biopsies and samples of the different biomaterials were solubilised by high-speed homogenization and subjected to negative staining and immunoelectron microscopy (Figure 2). Specimens were compared by high resolution FESEM (Figure 2A-D) and TEM (Figure 2E-L). C-E specimens (Figure 2B,F,J) demonstrated similar ultrastructural features as native collagen fibre bundles in dermis (Figure 2A,E,I). They consisted of tightly packed collagen patches with many regions of different fibre orientations. In C-GAG (Figure 2C,G,K) and C (Figure 2D,H,L), structures of varying thickness were observed, embedded in large

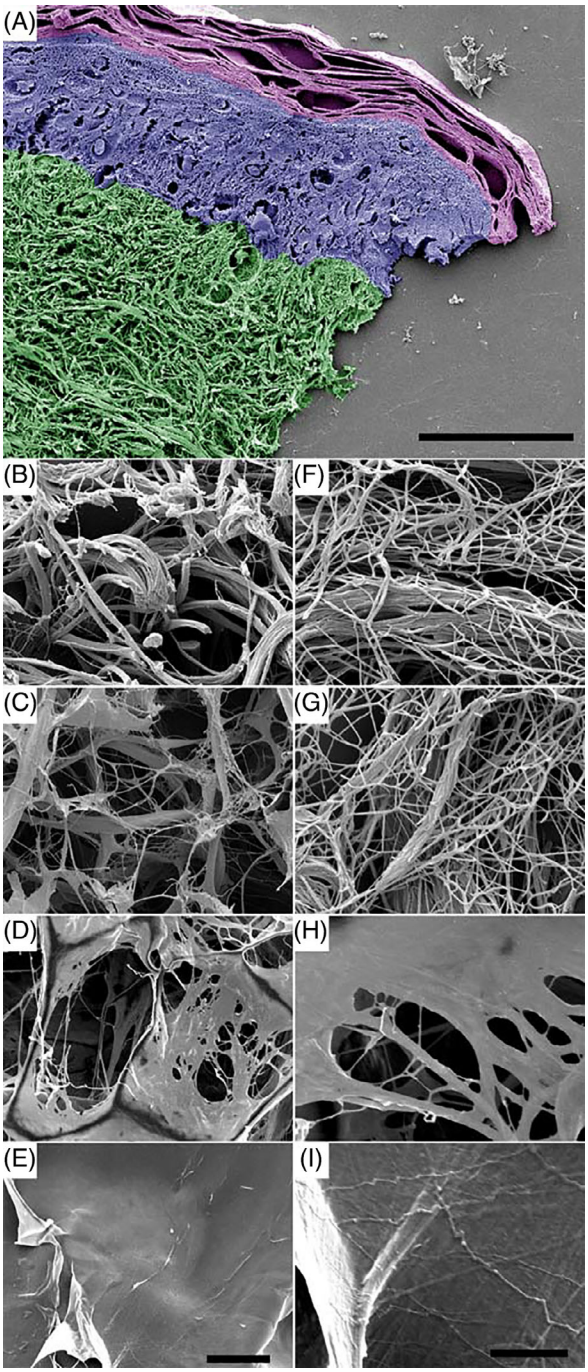

FIGURE 1 Ultrastructure of different biomaterials as compared with native human dermis. Specimens of human skin (A, B, F) were prepared for field emission scanning electron microscopy (FESEM) and compared with collagen elastin matrix C-E (C, G), bovine collagen matrix C-GAG (D, H), and porcine collagen matrix C (E, I). In (A), the stratum corneum is represented in magenta, the epidermis in blue, and the dermis in green pseudocolour, respectively. Note the appearance of extended fibrillar collagen networks in the dermis (B, C) and in C-E (F, G) and an abundance of amorphous sheets in C-GAG (D, E) and C (H, I). Left lane, low magnification overviews (500×); right lane, high magnification of the same area (10 000×). The scale bars represent 50 μm (A), 20 μm (B-E, left panel), and 5 μm (F-I, right panel)

amounts of an amorphous matrix. High-resolution TEM and immunostaining with gold-labelled antibodies against collagen III (arrowheads) and collagen V (arrows) and (Figure 2I-L) demonstrated native, mature, cross-striated collagen I fibrils with 63 nm-periodicity, containing associated collagens III and V in dermis (Figure 2I) and in C-E (Figure 2J). In contrast, in samples of C-GAG (Figure 2K) and C (Figure 2L), large fields of amorphous structures were

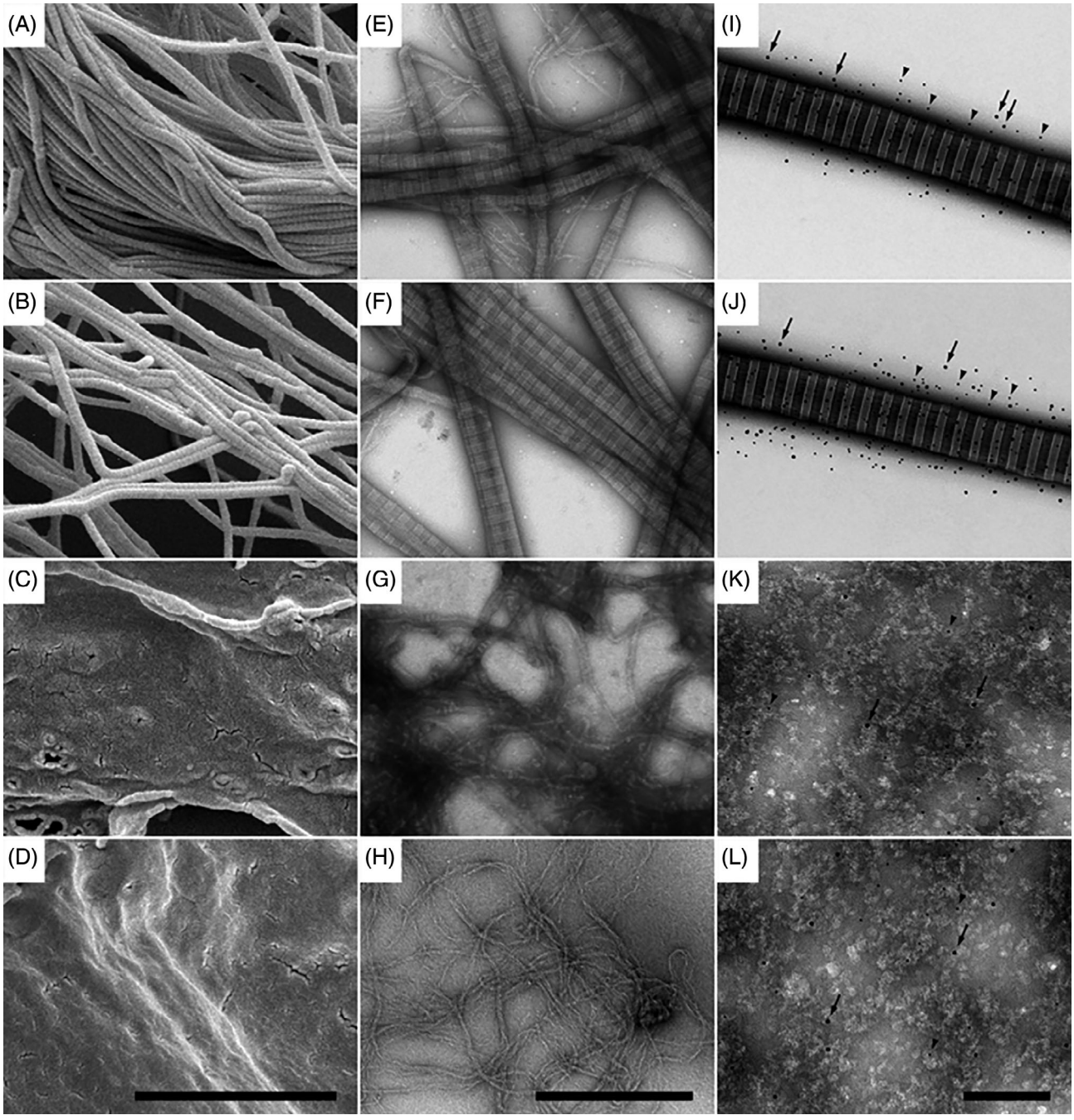

FIGURE 2 Ultrastructure and composition of different biomaterials as compared with native human dermis. Specimens of human dermis (A, E, I), C-E (B, F, J), C-GAG (C, G, K), and C (D, H, L) were visualised by field emission scanning electron microscopy (FESEM) at higher magnification (A-D), TEM (E-H), and immuno-TEM (I-L). Cross-striated fibrillar collagen structures with the characteristic 67 nm D-spacing pattern are visualised in dermis (A, E, I) and C-E (B, F, J) samples. In contrast, C-GAG (C, G, K) and C (D, H, L) specimens exhibit mixtures of microfibrillar and amorphous structures, lacking native cross striation patterns. (I-L), immuno-TEM at high magnification shows native cross-striated collagen I fibrils, containing large amounts of collagen III (5 nm Au, arrowheads) and collagen V (10 nm Au, arrows) in dermis (I) and C-E (J), whereas C-GAG (K) and C (L) contain sparse amounts and diffuse distributions of Au-particles. The sale bars represent 2 μm (A-D), 500 nm (E-H), and 200 nm (I-L)

observed, exhibiting no cross-striated collagen I fibrils and no specific immunodetection of collagens III and V.

3.2 | Native collagen fibrils in biological dermal templates promote cell adherence and cell spreading

The ability to attract skin fibroblasts and keratinocytes and to provide versatile cell attachment sites is a prerequisite for biological wound matrices in order to promote accelerated wound healing and epithelisation. Thus, we investigated whether the different wound matrices examined in this study exhibited similar properties. Samples of C-E (Figure 3A-C) were incubated with human skin fibroblasts. Specimens were then prepared for high resolution FESEM. A large number of fibroblasts (blue pseudocolour) were observed in firm adhesion to collagen fibrils (yellow pseudocolour) in C-E, exhibiting an elongated cell architecture. The plasma membrane was visible in intimate contact with the collagen fibrils (Figure 3B,C, arrows). Numerous filopodia were visualised emerging from the cell body, in firm contact with the collagen matrix and other cells (Figure 3B, arrowheads).

However, because of the intimate contact with the native collagen fibrils, the cells were frequently not readily structurally distinguishable from the underlying wound matrix. Therefore, for a quantitative assessment of cell architecture and adhesion parameters, the different wound matrices were sectioned, incubated with human fibroblasts and keratinocytes for appropriate times and subsequently prepared for FESEM. (Figure 3D-G) exhibits human skin fibroblasts growing on sections of human skin (D), C-E (E), C-GAG (F) and C (G) as visualised by FESEM. On native human skin (D) and C-E (E), an elongated and well spread-out cell architecture was predominant, whereas mostly rounded cell shapes were observed in C-GAG (F) and C (G).

3.3 | Quantitative assessment of cell adherence and architecture on native collagen fibrils

Biological wound matrix sections, mounted on microscopic slides, were incubated with fibroblasts (Figure 4A) and keratinocytes (Figure 4B). Adherent cells on different random locations were identified and quantified by FESEM for each wound dressing as shown in Figure 3. Fibroblasts and keratinocytes adhered to the different biomaterial surfaces at varying amounts and with different kinetics. Interestingly, the affinity of C-E surfaces for both cell types was comparatively high. Thus, the number of adhered fibroblasts

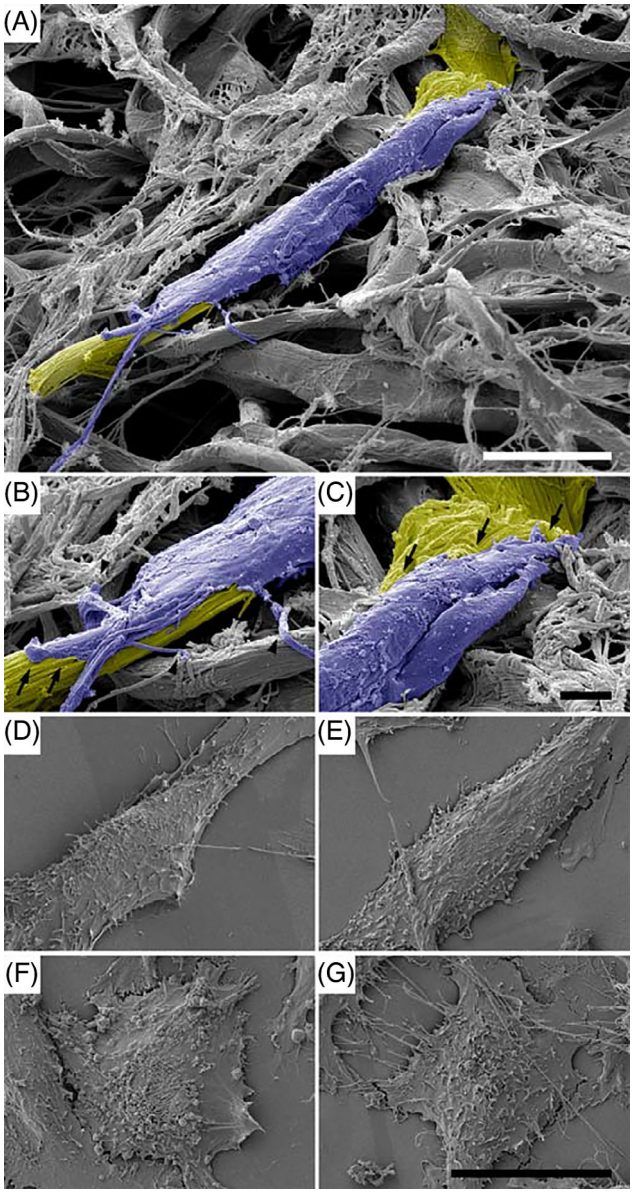

FIGURE 3 Characteristics of cell adherence to different biomaterials as visualised by field emission scanning electron microscopy (FESEM). A, C-E was incubated with human dermal fibroblasts. Fibroblasts (blue pseudocolour) adhere firmly to collagen fibrils (yellow pseudocolour) in C-E. The scale bar represents 10 μm. B, The leading edge and, C, the trailing edge of a fibroblast adhering to native collagen fibrils in C-E are shown at higher magnification. The plasma membrane is in intimate contact with the collagen (arrows). Numerous filopodia in contact with the collagen matrix and other cells are visible (arrowheads). The scale bar represents 20 μm. (D-G) Human skin fibroblasts growing on microscopic slides coated with homogenates of human skin (D), C-E (E), C-GAG (F), and C (G) are visualised by FESEM. Note the elongated cell architecture in (A, B) and the rounded cell shapes in (F, G). The scale bar represents 20 μm

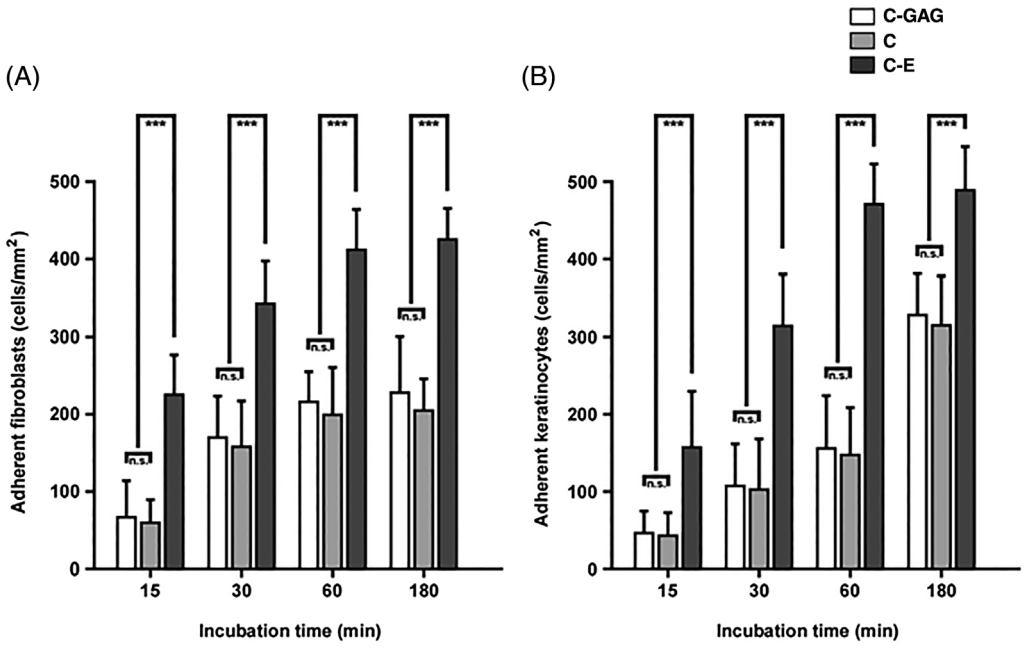

FIGURE 4 Quantitative evaluation of initial fibroblast and keratinocyte adherence to different biomaterials. Biomaterial sections, mounted on microscopic slides, were incubated with fibroblasts (A) of keratinocytes (B). Adhered cells were identified and counted by electron microscopy as shown in Figure 3. In each case, about 500 randomly selected electron micrographs were evaluated. Staples are given as means med SD error bars from three different experiments. Statistical significances are expressed as n.s. ($P \geq .05$); * ($P \leq .05$); ** ($P \leq .01$); *** ($P \leq .005$)

(Figure 4A) and keratinocytes (Figure 4B) increased significantly and steadily over time from 226 +/− 48 (15 minutes fibroblasts) and 108 +/− 71(15 minutes keratinocytes) to 424 +/− 43 (180 minutes fibroblasts) and 487 +/− 57 (180 minutes keratinocytes). In contrast, fibroblast and keratinocyte binding to both C-GAG and C appeared significantly lower in all examined time intervals, amounting from 72 +/− 47 (15 minutes fibroblasts C-GAG) and 68 +/− 29 (15 minutes fibroblasts C), and 49 +/− 24 (15 minutes keratinocytes C-GAG) and 46 +/− 26 (15 minutes keratinocytes C) to 227 +/− 73 (180 minutes fibroblasts C-GAG) and 208 +/− 42 (180 minutes fibroblasts C), and 329 +/− 43 (180 minutes keratinocytes C-GAG) and 215 +/− 59 (180 minutes keratinocytes C), respectively.

The quantitative evaluation of the influence of a given biological wound matrix on cellular architecture is shown in Figure 5. After 30 minutes incubation C-E, both fibroblasts and keratinocytes exhibited a significantly less circular morphology, were more spread and covered a larger area than cells on C-GAG and C. Similar observations were made in all time intervals, and finally, at the 180 minutes incubation end points, both cell types showed a considerably more pronounced fibroblast- and keratinocyte-characteristic cell architecture on C-E over C-GAG and C.

3.4 | Quantitative assessment of proliferation, viability, and alignment on native collagen fibrils

As a next step, we set out to correlate the ability of the different biomaterials to stimulate cell proliferation and growth. After seeding, the cells grew well on C-E and their proliferation, estimated by direct measurement in the FESEM, was significantly higher than on C-GAG and C in all time intervals (as denoted in Figure 6). A comparison of the cell behaviour on the different dermal templates showed that there was significantly higher cell proliferation on C-E than on the other biomaterials, mainly on day 14 after seeding. The cells were well spread and elongated through the native collagen fibril scaffold of C-E and tended to be polygonal and elongated in shape.

Notably, assessment of α-SMA expression by immunohistochemistry showed that the cells on C-E maintained their fibroblast phenotype to a high degree. In contrast, on C-GAG and C, the cells progressively exhibited a significant degree of smooth muscle phenotype during their cultivation.

Interestingly, the cells grown on C-E rapidly ingressed into the native collagen scaffolds and demonstrated a high degree of association and alignment with the collagen fibrils into elongated structures (Figure 7). By contrast, the different cell types adopted a more random orientation on C-GAG and C.

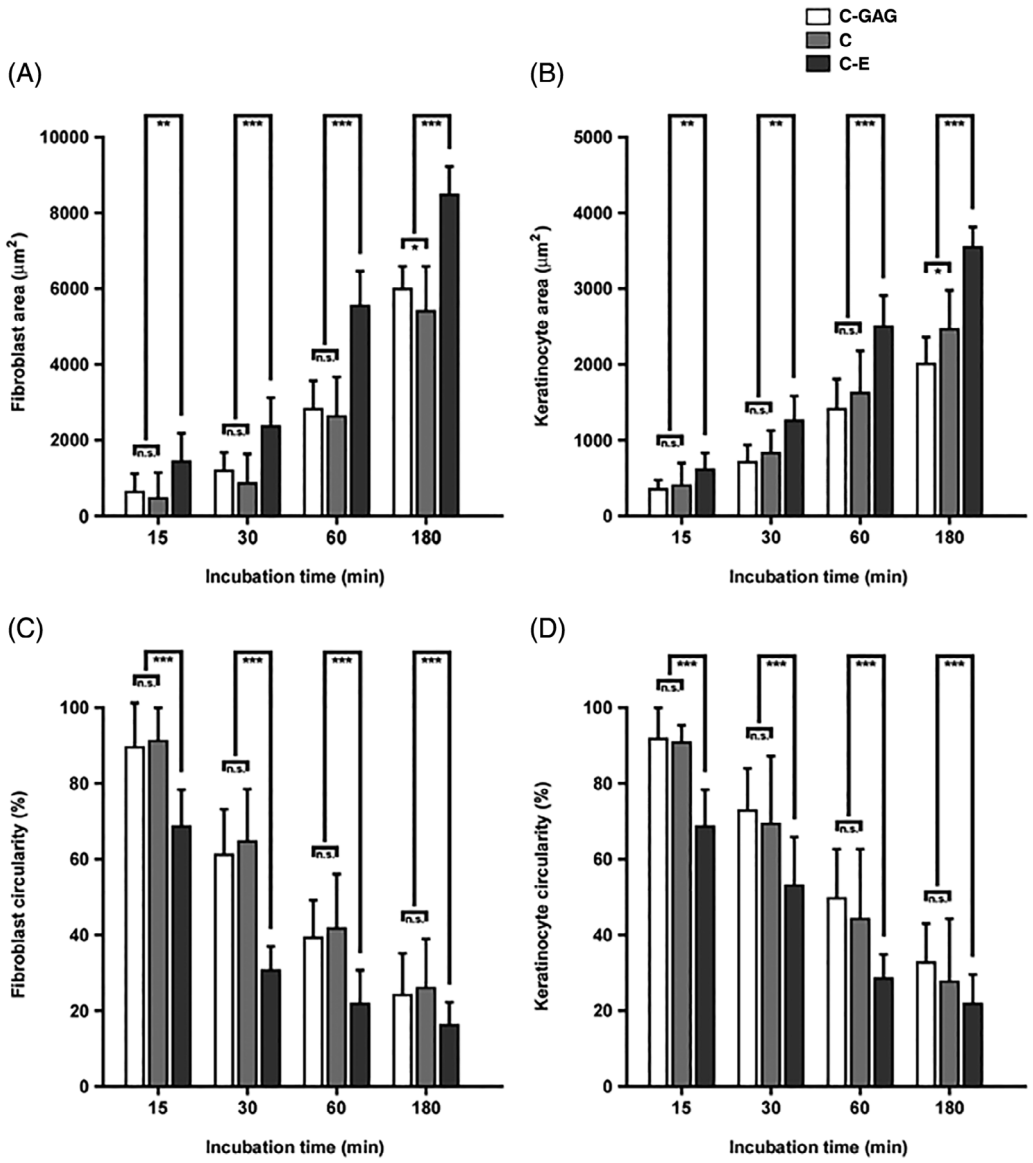

FIGURE 5 Quantitative evaluation of fibroblast and keratinocyte architecture on different biomaterials during initial adherence. Biomaterial sections were incubated with human fibroblasts (A, C) or keratinocytes (B, D) between 15 and 180 minutes. Cellular parameters such as cell area (A, B) and cell circularity (C, D) were determined on electron micrographs. In each case, about 500 cellular profiles were evaluated. Staples are given as means med SD error bars from three different experiments. Statistical significances are expressed as n.s. ($P \geq .05$); * ($P \leq .05$); ** ($P \leq .01$); *** ($P \leq .005$)

Taken together, the results of this study implicate that the native collagen fibril scaffolds found in C-E provide compatible surfaces for natural cell adherence, spreading, proliferation, and viability. Biomaterials with lesser amounts of native, intact collagen fibril networks appear to exhibit a less pronounced potential to harbour these properties.

4 | DISCUSSION

Wound healing is a carefully orchestrated and interactive process, relying on the coordination between extracellular matrix components, different cell types and their soluble mediators. The use of collagen for medical devices has been established for several decades. Collagen matrices are used in haemostasis, wound healing, and regenerative medicine, for example, as dermal templates. In order to create an optimal environment for cellular ingrowth, the nativity of collagen must be preserved. Brown et al conducted in vivo experiments in canine models to assess the influence of different ECM-based implants on the regeneration of surgical wounds. The results showed that natural wound matrices with a more native composition stimulated the formation of

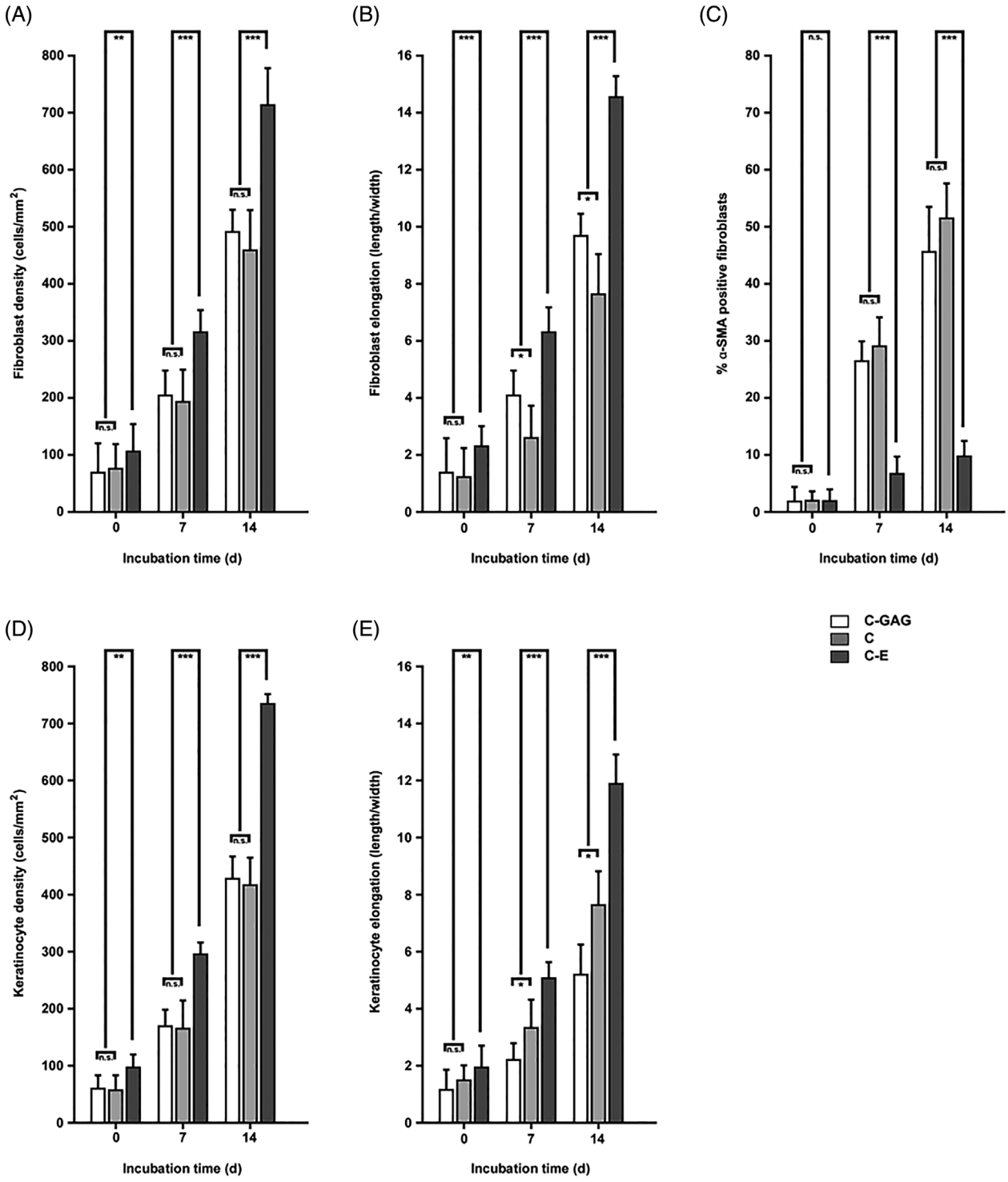

FIGURE 6 Quantitative evaluation of long-term fibroblast and keratinocyte proliferation and phenotype on different biomaterials. Biomaterial sections were incubated with human fibroblasts (A-C) or keratinocytes (D-F) and maintained in culture for 14 days. Cellular parameters such as cell density (A, D), cell elongation (B, E), and α-SMA positive cells were determined on electron micrographs. In each case, about 500 cellular profiles were evaluated. Staples are given as means med SD error bars from three different experiments. Statistical significances are expressed as n.s. ($P \geq .05$); * ($P \leq .05$); ** ($P \leq .01$); *** ($P \leq .005$)

site-appropriate and functional new tissues that resembled a native situation.[21-23]

We have recently demonstrated that the innate properties of such natural wound matrices regulate the proteolytic balance in the wound bed by binding and inactivating tissue proteases.[18] In the present study, by an integrated approach including high resolution field emission electron microscopy, we demonstrate that

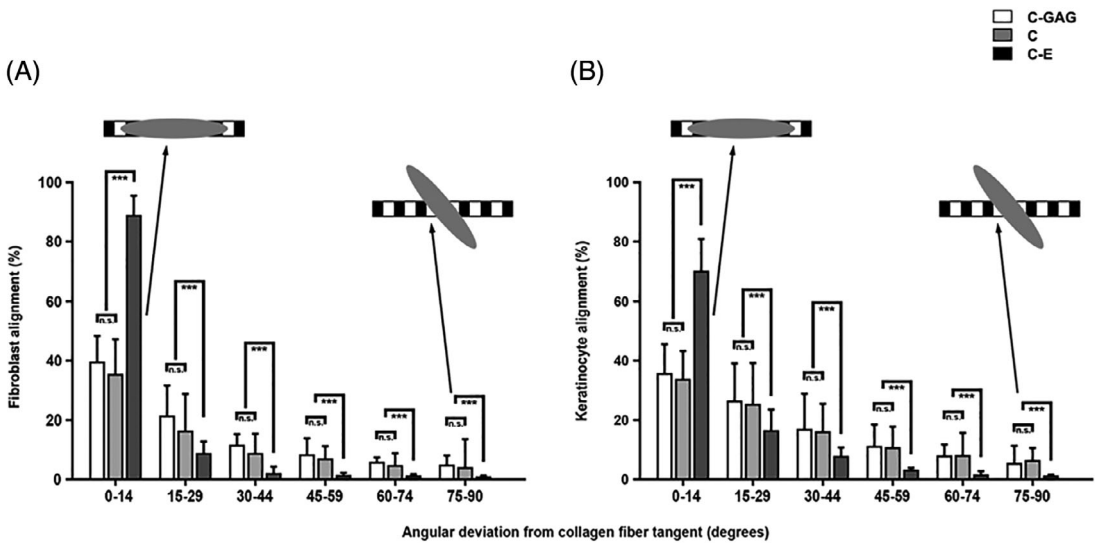

FIGURE 7 Quantitative evaluation of fibroblast and keratinocyte alignment on different biomaterials. Cell alignment was determined after 7 days of adhesion time. Deviations of 0° and 90° are the extreme points, where 0° corresponds to strict alignment and 90° corresponds to cell orientation perpendicular to collagen fibrils. Cells are more oriented on native collagen fibrils in C-E than cells on C-GAG and C. In each case, about 500 cellular profiles were evaluated. Staples are given as means med SD error bars from three different experiments. Statistical significances are expressed as n.s. ($P \geq .05$); * ($P \leq .05$); ** ($P \leq .01$); *** ($P \leq .005$)

native collagen scaffolds in biological wound matrices stimulate epidermal and dermal cell ingrowth, survival and proliferation and regulate myofibroblast differentiation. Our observations suggest that a stimulating effect on a cellular level because of this biomaterial is related to accelerated wound closure, re-epithelialisation and tissue regeneration, and thus the restoration of proper tissue functionality.

A variety of dermal matrices are commercially available that utilised different sources of materials and processing methodologies. These variations in starting material and processing are known to impact the biochemical and structural properties of the final scaffold and biological response.[24] All dermal matrices used in this study consist of bovine or porcine collagen by different manufacturing. However, in order to provide an optimal environment for cellular infiltration, morphology, and viability, the nativeness of the collagen in a biomaterial as well as its helical structures and cellular binding sides need to be retained.[25] Indeed, in the present work, we also found a strong variation in dermal cell ingrowth on the different collagen biomaterials. The observed variations were highly dependent on differences in the content of native, dermis-like collagen scaffolds, and could thus be attributed to the manufacturing process. The manufacturing process of C-E seems to ensure that a major part of the native collagen structure remains intact, a fact that is particularly important for the biocompatibility and cell colonisation properties of the material. Longitudinal orientation of collagen fibres within a given fibre bundle, and different orientations of fibre bundles with respect to each other, was ensured in order to mimic the natural dermis structure.

The fabrication of such native collagen fibre scaffolds is expected to enhance their functionality by mimicking both the mechanical and biological dermis environment and thus promote superior wound healing and tissue regeneration. These findings are in accordance with data reported by Böhm et al.[26] They showed in in vitro experiments that the importance of the manufacturing process and the ability to save the nativeness of collagen is more important for the performance of collagen matrices than the animal source of collagen. Killat et al[27] demonstrated recently that C-E skin substitutes resemble healthy skin in its three-dimensional morphology and integrity, confirming our results. Furthermore, when seeded or injected with skin cells, C-E sustains viable and proliferating cells throughout the entire matrix during a prolonged time, which is in accordance with our results. Importantly, clinical outcomes from the use of epidermal and dermal skin substitutes show that they are promising adjunctive tools for addressing soft tissue defects and have improved outcomes in reconstructive procedures.[28,29] Other clinical studies suggest that the use of dermal skin substitutes may be an alternative for flaps, or may be suitable for coverage of radial flap donor sites.[30-32] Thus, the experimental data confirmed that native collagen scaffolds provide desirable biomechanical, biochemical, and cell biological properties and represent a class of skin substitutes with superior tissue regeneration properties.

One of the main functions of collagen in wounds is the guidance of cell growth and migration during the proliferation and remodelling phase of the healing process.[33] These favourable properties for cell binding and growth make collagen a promising material for clinical application. Our study confirmed that successful cell attachment was possible on the native collagen-based dermal substitutes. High resolution FESEM showed that cell attachment was clearly visible on C-E already on day 0. The adhered cells rapidly aligned along the native collagen fibre bundles and started to exhibit a natural cell morphology. In contrast, initial pictures of C-GAG and C materials showed only a very sparse presence of cells, which frequently were poorly adhered and thus appeared more rounded. These observations suggest that cell adherence occurred at different speeds on the different materials. Rounded cells might have not yet been completely attached to some of the materials and were washed away during the sample preparation procedure. In contrast, elongated and well-oriented cells might represent viable and active, in accordance to previous work.[34]

Fibroblasts are important cell types in wound healing with their unique capability to produce matrix components, which are necessary for wound closure and replacement of the injured matrix. Keratinocytes on the other hand are important for re-epithelisation. Upon tissue injury, keratinocytes and fibroblasts become activated to proliferate in the peri-wound stroma and to transmigrate from the collagen-rich connective tissue into the wound provisional matrix of fibrin and fibronectin.[35,36] Their cross talk with other cell types participating in wound healing, and their extracellular microenvironment, are critical for successful tissue regeneration.[3,37] Importantly, a properly organised extracellular matrix network of collagen fibres, carbohydrates, and glycoproteins surrounding the cells, is the main regulator in cellular function and tissue regeneration.

Correspondingly, cell ingrowth and adherence, cell migration, and cell function in the wound bed are greatly influenced by the pore size, composition, and nativeness of the dermal substitute.[3,37] In our study, after incubating fibroblasts and keratinocytes on C-E containing native collagen fibrils, cell adherence, morphology, and viability parameters were increased as compared with other biomaterials, indicating that C-E is both biocompatible and a stimulatory material for skin cells. The stimulatory effect sustained after longer time incubation. Thus, our results demonstrate that C-E with its content of native collagen fibrils creates an environment ideal for cell function and natural wound healing. In addition, the native bovine dermal collagen containing type I, III and V collagens, similar to human tissues, is particularly suitable as an extracellular scaffold for tissue regeneration. Compared with C-E, C-GAG and C are chemically cross-linked with glutaraldehyde. Although crosslinking can be used to improve matrix longevity in the wound area, the crosslinking can also have detrimental effects on wound healing processes. For example, de Vries et al[38] demonstrated in a full-thickness porcine model that a glutaraldehyde cross-linked collagen matrix induced a foreign body response compared with non-cross-linked collagen matrix, which in the end negatively affected the dermis formation and contraction outcome parameter. Additionally, Middelkoop et al demonstrated in in vitro experiments that cross-linked collagen matrices are cytotoxic and do not allow cell proliferation on the matrix.[39]

Importantly, fibroblasts adhered to the native collagen fibre bundles in C-E exhibited a diminished number of myofibroblast phenotypes as compared with the other examined biomaterials. These findings are in accordance with[35,36] where the treatment of full thickness skin wounds with native collagen matrices resulted in reduced numbers of myofibroblasts and reduced wound contraction. Although myofibroblasts play an important role in the wound healing process, excessive presence of myofibroblasts can lead to increased contraction and collagen deposition resulting in hypertrophic scar formation.[40,41] In addition, chemical cross-linking can lead to increase matrix rigidity, which is an important factor in myofibroblast differentiation.[41] The results in this and the other studies discussed here can be interpreted as a more physiologic tissue regeneration occurring at the host/biomaterial interface. The fibrillar structure of the native collagen matrix will function as natural scaffolds and guidance ridges for collagen- and extracellular matrix-producing cells and stimulates the formation of mature collagen fibres in the regenerating dermis. This will finally result in less aberrant scar tissue formation and contractures in the healing wound, because of the regeneration of physiologic new connective tissue and dermis structures.[7] These results are in accordance with clinical in vivo results, demonstrating significant improved skin quality and elasticity, quality of scar tissue and dermal architecture upon the treatment of burns with dermal substitutes containing native collagen fibrils.[42,43] These results are also in accordance with other clinical studies on patients with impaired mobility resulting from burn sequelae. The data demonstrated improved scar skin quality, improved rate of mobility recovery, and best performance in retraction rate upon treatment with native collagen dermal templates.[44]

Our in vitro findings are intended to give an estimation of the behaviour of the dermal templates in a wound. There seems to be a connection between nativity of collagen and cellular behaviour. But it has to be considered that in vivo a more complex set of different cell types, bodily fluids, possible microbial contamination, and

mechanic agitation influences the wound healing process and with this the performance of dermal substitutes. Therefore, it will be relevant and interesting to elucidate further the influence of inflamed in vivo wound healing environments on the interplay of dermal templates and different cell types involved in the wound healing process.

Taken together, we conclude that dermal substitution of full-thickness skin defects with biological wound dressings like C-E lead to an improved wound environment. The native dermis-like collagen fibrillar networks exhibit premium properties for cell ingrowth, survival, and proliferation. They form scaffolds that guide fibroblasts, keratinocytes, and possibly other cells towards their physiologic locations in the healing wound. By balancing the expression of myofibroblasts, they lead to decreased wound contraction and aberrant scar formation. Biological dermal regeneration templates with native collagen scaffolds may thus be beneficial for the management of full-thickness skin defects and the restoration of normal structure and function.

ACKNOWLEDGEMENTS

The matrix Matriderm® was supplied by MedSkin Solutions Dr. Suwelack AG, Billerbeck, Germany. We are grateful to the staff in the BioEM Lab, Biozentrum, University of Basel, the Microscopy Facility at the Department of Biology, Lund University, and the Core Facility for Integrated Microscopy (CFIM), Panum Institute, University of Copenhagen, for providing highly innovative environments for electron microscopy. We thank Cinzia Tiberi (BioEM lab), Maria Baumgarten (BMC, Lund) and Ola Gustafsson (Microscopy Facility) for skillful work, Carola Alampi (BioEM lab), Mohamed Chami (BioEM lab) and Klaus Qvortrup (CFIM) for practical help with electron microscopy. This work was supported by grants from the Swedish Research Council (project 7480), the Swedish Foundation for Strategic Research (K2014-56X-13413-15-3), the Foundations of Crafoord, Johan and Greta Kock, Alfred Österlund, King Gustav V Memorial Fund, and the Medical Faculty at Lund University.

CONFLICT OF INTEREST

The authors declare that they have no conflicts of interest with the contents of this article.

ORCID

Matthias Mörgelin https://orcid.org/0000-0002-6212-6990

REFERENCES

1. Lo CH, Chong E, Akbarzadeh S, Brown WA, Cleland H. A systematic review: current trends and take rates of cultured epithelial autografts in the treatment of patients with burn injuries. *Wound Repair Regen*. 2019;27:693-701.
2. Zhou H, You C, Wang X, et al. The progress and challenges for dermal regeneration in tissue engineering. *J Biomed Mater Res A*. 2017;105:1208-1218.
3. Shah JMY, Omar E, Pai DR, Sood S. Cellular events and biomarkers of wound healing. *Indian J Plast Surg*. 2012;45:220-228.
4. Urciuolo F, Casale C, Imparato G, Netti PA. Bioengineered skin substitutes: the role of extracellular matrix and vascularization in the healing of deep wounds. *J Clin Forensic Med*. 2019;8:E2083.
5. Nour S, Baheiraei N, Imani R, et al. A review of accelerated wound healing approaches: biomaterial-assisted tissue remodeling. *J Mater Sci Mater Med*. 2019;30:120.
6. Bacakova M, Pajorova J, Broz A, et al. A two-layer skin construct consisting of a collagen hydrogel reinforced by a fibrin-coated polylactide nanofibrous membrane. *Int J Nanomedicine*. 2019;14:5033-5050.
7. Abou Neel EA, Bozec L, Knowles JC, et al. Collagen—emerging collagen based therapies hit the patient. *Adv Drug Deliv Rev*. 2013;65:429-456.
8. An B, Lin YS, Brodsky B. Collagen interactions: drug design and delivery. *Adv Drug Deliv Rev*. 2016;97:69-84.
9. Parenteau-Bareil R, Gauvin R, Berthod F. Collagen-based biomaterials for tissue engineering applications. *Dent Mater*. 2010;3:1863-1887.
10. Chattopadhyay S, Raines RT. Review collagen-based biomaterials for wound healing. *Biopolymers*. 2014;101:821-833.
11. Baum CL, Arpey CJ. Normal cutaneous wound healing: clinical correlation with cellular and molecular events. *Dermatol Surg*. 2005;31:674-686.
12. Ghica MV, Albu Kaya MG, Dinu-Pîrvu CE, Lupuleasa D, Udeanu DI. Development, optimization and in vitro/in vivo characterization of collagen-dextran spongious wound dressings loaded with flufenamic acid. *Molecules*. 2017;22:1552.
13. Guo R, Lan Y, Xue W, et al. Collagen-cellulose nanocrystal scaffolds containing curcumin-loaded microspheres on infected full-thickness burns repair. *J Tissue Eng Regen Med*. 2017;11:3544-3555.
14. Bhowmick S, Thanusha AV, Kumar A, Scharnweber D, Rother S, Koul V. Nanofibrous artificial skin substitute composed of mPEG–PCL grafted gelatin/hyaluronan/chondroitin sulfate/sericin for 2nd degree burn care: *in vitro* and *in vivo* study. *RSC Adv*. 2018;8:16420-16432.
15. Yoon D, Yoon D, Cha HJ, Lee JS, Chun W. Enhancement of wound healing efficiency mediated by artificial dermis functionalized with EGF or NRG1. *Biomed Mater*. 2018;13:045007.
16. Powell HM, Supp DM, Boyce ST. Influence of electrospun collagen on wound contraction of engineered skin substitutes. *Biomaterials*. 2008;29:834-843.
17. Linder A, Johansson L, Thulin P, et al. Erysipelas caused by group a streptococcus activates the contact system and induces the release of heparin-binding protein. *J Invest Dermatol*. 2010;130:1365-1372.
18. Tati R, Nordin S, Abdillahi SM, Mörgelin M. Biological wound matrices with native dermis-like collagen efficiently modulate protease activity. *J Wound Care*. 2018;27:199-209.
19. Bober M, Enochsson C, Collin M, Mörgelin M. Collagen VI is a subepithelial adhesive target for human respiratory tract pathogens. *J Innate Immun*. 2010;2:160-166.
20. Baschong W, Wrigley NG. Small colloidal gold conjugated to fab fragments or to immunoglobulin G as high-resolution

labels for electron microscopy: a technical overview. *J Electron Microsc Tech*. 1990;14:313-323.
21. Brown BN, Chung WL, Pavlick M, et al. Extracellular matrix as an inductive template for temporomandibular joint meniscus reconstruction: a pilot study. *J Oral Maxillofac Surg*. 2011;69:e488-e505.
22. Brown BN, Chung WL, Almarza AJ, et al. Inductive, scaffold-based, regenerative medicine approach to reconstruction of the temporomandibular joint disk. *J Oral Maxillofac Surg*. 2012;70:2656-2668.
23. Bush K, Gertzman AA. Process development and manufacturing of human and animal acellular dermal matrices. *Skin Tissue Engineering and Regenerative Medicine*. Amsterdam, NL: Academic Press; 2016:83-108.
24. International consensus. *Acellular Matrices for the Treatment of Wounds. An Expert Working Group Review*. London, UK: Wounds International; 2010.
25. Brett DA. Review of collagen and collagen-based wound dressings. *Wounds*. 2008;20:347-356.
26. Böhm S, Strauss C, Stoiber S, Kasper C, Charwat V. Impact of source and manufacturing of collagen matrices on fibroblast cell growth and platelet aggregation. *Materials (Basel)*. 2017;10:1086.
27. Killat J, Reimers K, Choi CY, Jahn S, Vogt PM, Radtke C. Cultivation of keratinocytes and fibroblasts in a three-dimensional bovine collagen-elastin matrix (MatriDerm®) and application for full thickness wound coverage *in vivo*. *Int J Mol Sci*. 2013;14:14460-14474.
28. Lucich EA, Rendon JL, Valerio IL. Advances in addressing full-thickness skin defects: a review of dermal and epidermal substitutes. *Regen Med*. 2018;13:443-456.
29. Nicoletti G, Tresoldi MM, Malovini A, Visaggio M, Faga A, Scevola S. Versatile use of dermal substitutes: a retrospective survey of 127 consecutive cases. *Indian J Plast Surg*. 2018;51:46-53.
30. Gümbel D, Ackerl M, Napp M, et al. Retrospective analysis of 56 soft tissue defects treated with one-stage reconstruction using dermal skin substitutes. *J Dtsch Dermatol Ges*. 2016;14:595-601.
31. Cristofari S, Guenane Y, Atlan M, Hallier A, Revol M, Stivala A. Coverage of radial forearm flap donor site with full thickness skin graft and Matriderm®: An alternative reliable solution? *Ann Chir Plast Esthet*. 2019;S0294-1260(19)30097-4.
32. Watfa W, di Summa PG, Meuli J, Raffoul W, Bauquis O. MatriDerm decreases donor site morbidity after radial forearm free flap harvest in transgender surgery. *J Sex Med*. 2017;14(10):1277-1284.
33. Masci VL, Taddei AR, Gambellini G, Giorgi F, Fausto AM. Ultrastructural investigation on fibroblast interaction with collagen scaffold. *J Biomed Mater Res A*. 2016;104:272-282.
34. Arbi S, Eksteen EC, Oberholzer HM, Taute H, Bester MJ. Premature collagen fibril formation, fibroblast-mast cell interactions and mast dell-mediated phagocytosis of collagen in keloids. *Ulstrastruct Pathol*. 2015;39:95-103.
35. De Vries HJC, Middelkoop E, Mekkes JR, Dutrieux RP, Wildevuur CHR, Westerhof W. Dermal regeneration in native non-cross-linked collagen sponges with different extracellular matrix molecules. *Wound Repair Regen*. 1994;2:37-47.
36. Spronk I, Polinder S, Haagsma JA, et al. Patient-reported scar quality of adults after burn injuries: a five-year multicenter follow-up study. *Wound Repair Regen*. 2019;27:406-414.
37. Bainbridge P. Wound healing and the role of fibroblasts. *J Wound Care*. 2013;22:410-412.
38. De Vries HJ, Mekkes JR, Middelkoop E, Hinrichs WL, Wildevuur CHR, Westerhof W. Dermal substitutes for full-thickness wounds in a one-stage grafting model. *Wound Repair Regen*. 1993;1:244-252.
39. Meuli M, Hartmann-Fritsch F, Hüging M, et al. A cultured autologous dermo-epidermal skin substitute for full-thickness skin defects: a phase I, open, prospective clinical trial in children. *Plast Reconstr Surg*. 2019;144:188-198.
40. Kattan WM, Alarfaj SF, Alnooh BM, et al. Myofibroblast-mediated contraction. *J Coll Physicians Surg Pak*. 2017;27:38-43.
41. Hinz B. Myofibroblasts. *Exp Eye Res*. 2016;142:56-70.
42. Ryssel H, Germann G, Kloeters O, Gazyakan E, Radu CA. Dermal substitution with MatriDerm(®) in burns on the dorsum of the hand. *Burns*. 2010;36:1248-1253.
43. Cervelli V, Brinci L, Spallone D, et al. The use of MatriDerm® and skin grafting in post-traumatic wounds. *Int Wound J*. 2011;8:400-405.
44. Hur GY, Seo DK, Lee JW. Contracture of skin graft in human burns: effect of artificial dermis. *Burns*. 2014;40:1497-1503.

How to cite this article: Dill V, Mörgelin M. Biological dermal templates with native collagen scaffolds provide guiding ridges for invading cells and may promote structured dermal wound healing. *Int Wound J*. 2020;17:618–630. https://doi.org/10.1111/iwj.13314